N. E. Dowling[1]

Fatigue Failure Predictions for Complicated Stress-Strain Histories

REFERENCE: Dowling, N. E., "**Fatigue Failure Predictions for Complicated Stress-Strain Histories,**" *Journal of Materials*, JMLSA, Vol. 7, No. 1, March 1972, pp. 71–87.

ABSTRACT: A cumulative fatigue damage procedure that considers sequence and mean stress is proposed for engineering metals. Fatigue life data for prestrained specimens are used to account for sequence effects due to crack initiation. Histories with fluctuating mean stress are analyzed by determining the mean stress of each cycle. The rain flow cycle counting method, which counts all closed stress-strain hysteresis loops as cycles, is employed in the damage procedure.

Axially loaded unnotched specimens of 2024-T4 aluminum were tested to failure using various complicated stress or strain control conditions. Life predictions using the proposed cumulative damage procedure were made prior to testing for 83 specimens. The predicted lives were within a factor of three of the actual lives for all of the tests and within a factor of two for more than 90 percent of the tests. In some of the tests there were large plastic strains, and in others the strains were predominantly elastic. Some of the stress control histories were similar to the load histories for actual machines, vehicles, and aircraft in that there were irregular loadings superimposed on changes in the static level.

It is shown that the use of the average mean stress to make life predictions can result in large nonconservative errors. The rain flow cycle counting method allows satisfactory predictions of the effects of different block sizes, different sequences of applying the same strain peaks, and superimposed loadings. The range pair counting method is nearly identical to the rain flow method, but the use of any of the other well known cycle counting methods, such as peak counting, level crossing counting, or range counting, can result in large differences between predicted and actual fatigue lives.

KEY WORDS: metals, aluminum alloys, stress-strain diagrams, failure, fatigue (materials), damage, crack initiation, fatigue life, stress cycle, axial stress, cyclic loads, strains, plastic deformation

Nomenclature

- Block — A sequence of straining or stressing that is repeatedly applied to a specimen until failure occurs
- ϵ — Strain measured on the gage length of a smooth specimen
- $\Delta\epsilon$ — Strain range
- $\Delta\epsilon_1$ — Total strain range during one complete block
- $\Delta\epsilon_2$ — Minor strain range
- $\Delta\epsilon_{rs}$ — The maximum strain range during one repetition of the random sequence in strain control
- j — The number of repetitions of the random sequence between changes in the static stress level
- k — Minor cycles per block; where the control consists of two superimposed signals of different frequencies, k is also the ratio of the higher frequency to the lower
- n — Number of cycles applied during the fatigue life at a given strain amplitude and mean stress
- N_f — Cycles to failure
- N_o — Cycles reduction in life due to prestraining
- N_p — Cycles to failure for a prestrained specimen
- $\frac{n}{N_f}$ — Ratio of cycles applied at a certain strain amplitude and mean stress to the expected life for a test at that level run to failure
- σ — Load per unit area for a smooth specimen
- $\Delta\sigma$, $\Delta\sigma_1$, $\Delta\sigma_2$ — Stress ranges similarly defined as for strain
- $\Delta\sigma_{rs}$ — The maximum stress range during one repetition of the random sequence in stress control
- σ_o — Mean stress
- $\Delta\sigma_o$ — Range of variation of the mean stress
- σ_{ave} — Average mean stress

A cumulative damage procedure is developed to predict the fatigue failure of engineering metals subjected to complicated stress-strain histories. Histories with plastic strainings and cycles not completely reversed in stress are considered.

Most previous workers in the area of cumulative damage have employed notched or bending members as test specimens. In such members the stresses and strains at the location of the fatigue failure are related to the applied loads in a complicated nonlinear manner [*1*, *2*] and are usually unknown. The two variables most significant in determining fatigue life can therefore not be isolated for study. In this investigation the relationship between stress-strain behavior and fatigue life is investigated for unnotched axially loaded specimens for which the stresses and strains can be measured for the duration of all tests. Since either the stress history or the strain history was known before each test was conducted, the other could be estimated and a life prediction made.

Simple linear summation of cycle ratios based on strain amplitude is illustrated in Fig. 1. Failure predictions made on this basis are often in error because sequence effects and mean stresses are not accounted for. For some stress-strain histories it is difficult to define a cycle, and some method of cycle counting must be employed. The simple procedure of Fig. 1 is modified and extended to make it consistent with existing fatigue data and to make it applicable to complicated stress-strain histories. The resulting more general cumulative damage procedure is used to make life predictions for a wide variety of complicated history tests on 2024-T4 aluminum.

Literature Survey

In this section the literature that relates to predicting fatigue lives from stress-strain histories is surveyed. Sequence effects,

[1]Research associate, Department of Theoretical and Applied Mechanics, University of Illinois, Urbana.

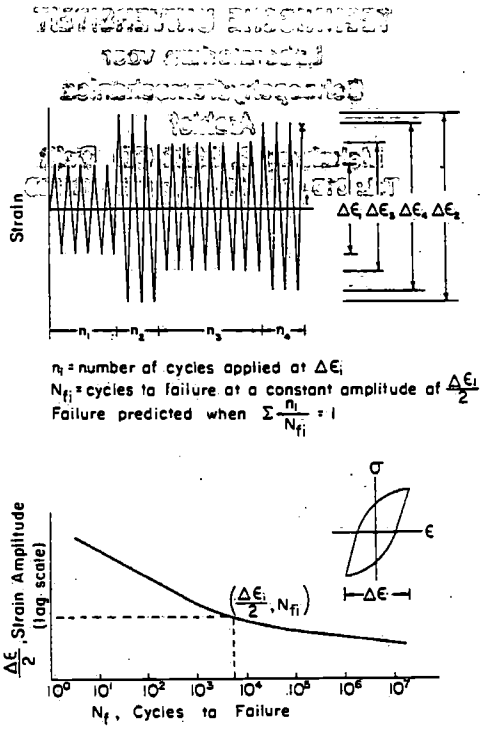

FIG. 1—*Fatigue failure predictions by linear summation of cycle ratios based on strain amplitude.*

especially the high-low effect due to crack initiation, are discussed. The various methods of counting cycles and of handling mean stresses are reviewed. Cyclic stress-strain response is treated briefly. At several points during the literature survey, conclusions are stated which contribute to the proposed cumulative damage procedure. The reader may omit this section without serious loss of continuity if he is familiar with the topics covered.

Sequence Effects

Crack initiation is defined as that portion of fatigue life prior to the existence of a tensile mode crack across several grains. For strengthened aluminum alloys and steels the initiation period is observed [*3–8*] to be short in the low cycle region, most of the life being spent in crack propagation. At longer lives an increasingly smaller fraction of the life is spent in propagation,

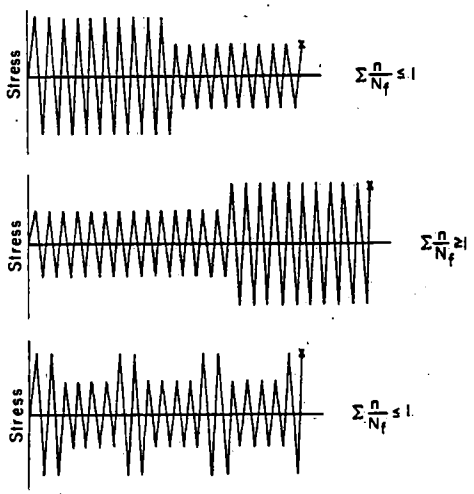

FIG. 2—*Sequence effects due to crack initiation.*

TABLE 1—*Cycle counting methods.*

Name	Example	Description
Peak	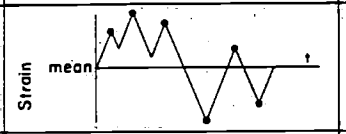	All maximums above the mean and all minimums below the mean are counted.
Mean crossing peak	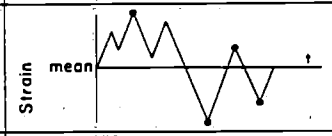	Only the largest peak between successive crossings of the mean is counted.
Level crossing	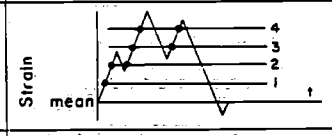	All positive slope level crossings above the mean, and negative slope level crossings below the mean, are counted.
Fatigue-meter	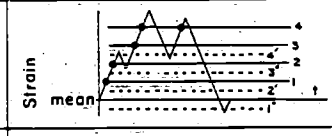	Similar to level crossing except that only one count is made between successive crossings of a lower level associated with each counting level.
Range	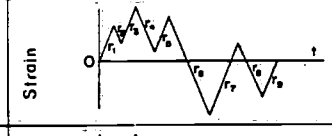	Each range, i.e. the difference between successive peak values, is counted as 1/2 cycle, the amplitude of which is half the range.
Range-mean	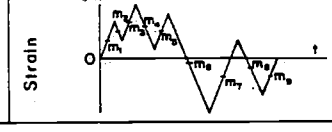	Ranges are counted as above and the mean value of each range is also considered.

until at long lives most of the fatigue life is required for crack initiation.

These observations on crack initiation explain the sequence effects [*9, 10*] shown schematically in Fig. 2. The deviations from linear summation of cycle ratios indicated in Fig. 2 are more pronounced when the difference between the two levels is larger [*11*]. For the high-low sequence, a crack that would ordinarily take many cycles to initiate at the low level can be initiated during the high level. Failure then occurs after fewer cycles at the low level than predicted. The high-low effect can be drastic [*12*] if the high level is in the low cycle region and the

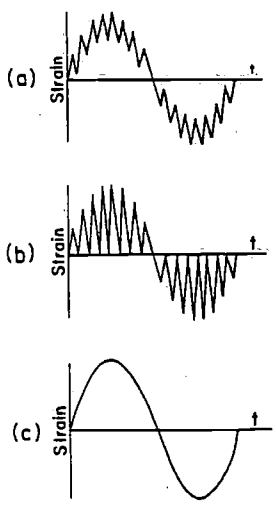

FIG. 3—*Sequences which cause problems for several cycle counting methods.*

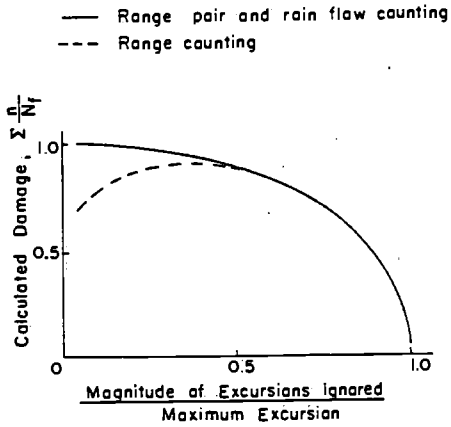

FIG. 4—*The effect of ignoring all excursions smaller than a specified value.*

low level is in the long life region. For the low-high sequence, the cycles at the low level are spent in initiating a crack that would have been initiated soon after the beginning of the high level even if they had not been applied. A large number of cycles at the low level can therefore be applied without significantly affecting the number of cycles required for failure at the high level. Damage summations greater than two are not possible for this low-high effect, because failure is expected if the constant amplitude fatigue life at either level is exceeded. Multiple changes in level are similar to the high-low sequence in that a crack initiated at the high level can propagate at the low level. The sequence effects of Fig. 2 do not occur if all of the levels cause significant plastic straining [*13–17*], which is consistent with the observation that the initiation period is short in the low cycle region.

Grover [*18*] proposed that the sequence effects due to crack initiation be accounted for using linear summation of cycle ratios separately over the initiation and propagation periods. He showed that this is the simplest damage rule that is mathematically possible for multilevel tests where the fraction of the fatigue life required for crack initiation is not constant for the different levels. Topper and Sandor [*12*] used constant amplitude data on specimens prestrained for 10 cycles at ± 0.02 to calculate the damage for all cycles after significant plastic straining occurred. Summations of cycle ratios close to unity were obtained for a wide variety of low-high, high-low, and two-level repeated block tests on both 2024-T4 aluminum and SAE 4340 steel.

In view of the crack initiation studies cited above [*3–8*], it is likely that the prestraining done by Topper and Sandor [*12*] was sufficient to cause crack initiation. If this assumption is made, the damage procedure used by Topper and Sandor is essentially equivalent to the damage rule proposed by Grover [*18*]. Linear summation of cycle ratios should give summations of cycle ratios close to unity for prestrained specimens only if prestraining causes crack initiation. Grover's damage rule and the assumption that prestraining causes crack initiation will be used in the proposed cumulative damage procedure.

There are other important sequence effects. Different sequences of straining can affect the fatigue life because different mean stresses are induced or because different amounts of plastic strain occur. These effects will be treated in detail later in this paper. Due to the coaxing effect [*19*], which occurs in strain aging metals, damage summations much greater than unity can be obtained by gradually increasing the stress amplitude from below the endurance limit. Coaxing will not be considered here, because 2024-T4 aluminum does not strain age and because the effect of coaxing is probably small even for strain aging metals, if the load history is irregular [*10*]. Initial plastic straining usually causes rapid cyclic softening or hardening, depending on the material, which may alter the stable stress-strain hysteresis behavior at subsequent lower levels. This effect is not thought to be important for 2024-T4, because no significant dependence of the stable behavior on the previous history has been observed.

Cycle Counting

Six well known cycle counting methods [*20, 21*] are described in Table 1. The range pair [*21, 22*] and the rain flow [*23*] counting methods are described and compared in the Appendix.

If the various cycle counting methods are compared on the basis of their applicability to complicated strain histories, it is easily seen that for most of them there are situations where unreasonable results are obtained. In the sequence shown in Fig. 3*a*, the small reversals do some fatigue damage that may or may not be significant compared to the damage done by the large cycle on which they are superimposed. Peak counting gives the same result for *a* and *b* of Fig. 3, but *b* is likely to be more damaging than *a*. Mean crossing peak counting gives the result that *a* is equivalent to *c*, which is nonconservative in cases where the small reversals do significant damage.

The range and range mean counting methods have the characteristic that, if small reversals are counted, the large ranges are broken up and counted as several smaller ones. This gives the unrealistic result that small excursions do negative damage, as the calculated damage can be decreased by including them (see Fig. 4). For example, in Fig. 3*a* the large cycle on which the smaller ones are superimposed is not recognized by range counting; therefore, the calculated damage could easily be less than for Fig. 3*c*. The range pair and rain flow counting results are much more reasonable, the small reversals being treated as interruptions of the larger strain ranges, and the damages for the large and small strain ranges are simply added.

No information whatever is given on sequence by the peak, mean crossing peak, level crossing, or Fatiguemeter counting methods. These methods all give the same counting result for *a* and *b* of Fig. 5. Some fatigue damage calculations for sequences similar to these two, using simple linear summation of cycle ratios as illustrated in Fig. 1 and the strain-life curve for any structural metal, will show that *b* is expected to be much more damaging than *a*. In Fig. 6, *a* and *b* are identical except that the signs of the smaller peaks are opposite. The peaks and level crossing are the same for these two sequences, but the range pair and rain flow counting methods predict that *a* will be more damaging than *b*. It will be experimentally shown that *a* will cause more plastic straining than *b* and that the fatigue lives can be significantly different.

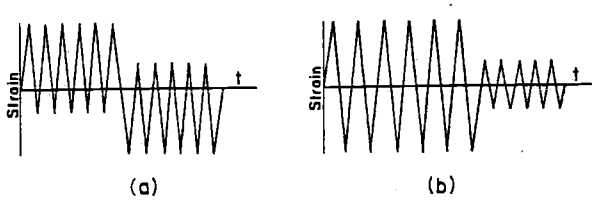

FIG. 5—*Two sequences for which several counting methods give the same result.*

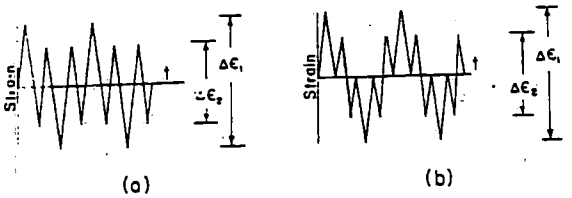

FIG. 6—*A change in sequence that can affect the fatigue life.*

All of the counting methods, with the exception of the range pair and rain flow methods, have been shown to have serious flaws. The comparison of these two counting methods in the Appendix shows that they are nearly identical. No test could be devised for which either gave an unreasonable life prediction. The rain flow method applied to a strain history gives information on the stress response in that all closed stress-strain hysteresis loops are counted as cycles.

Mean Stress

In stress-strain histories where large mean stresses are present for a significant number of cycles, the fatigue life cannot be adequately predicted without considering the effect of mean stress. Tensile mean stresses shorten the fatigue life, and compressive mean stresses prolong it.

The basic cause of the effect of mean stress is not known. Some of the possibilities are that mean stress affects the stable stress-strain behavior, the rate of crack initiation, the size of shear crack necessary to start a normal mode crack, the crack propagation rate, and the crack size necessary to cause final failure. Several of these possibilities are explored in the test results to be presented, but it is probably not possible to thoroughly investigate the effect of mean stress without making extensive microscopic studies.

Simple linear summation of cycle ratios (Fig. 1) can be extended to include the effect of mean stress if constant amplitude fatigue life data at different values of mean stress are available. Such data can be used to plot strain-life curves for various values of mean stress, and the fatigue life for any desired combination of mean stress and strain amplitude can be found by interpolating between these curves.

Several methods for predicting the effect of mean stress on fatigue life have been proposed [*12*, *24–27*]. Three of these, expressed as parameters that can be plotted versus cycles to failure and that should bring data for various mean stresses all onto one line, are as follows:

a. $\dfrac{\Delta\sigma/2}{1 - \sigma_o/S_u}$ Smith [*24*]

b. $\dfrac{\Delta\sigma/2}{1 - \sigma_o/\sigma_f'}$ Morrow [*26*]

c. $[(\sigma_o + \Delta\sigma/2)\ (\Delta\epsilon/2)E]^{1/2}$ Smith, Watson, and Topper [*27*]

In these parameters, the ultimate tensile strength, S_u, and the modulus of elasticity, E, are defined in the usual manner. The quantity σ_f', which is approximately equal to the true fracture strength, is defined in Ref *26*. Note that the above parameters reduce to stress amplitude when the mean stress is zero and the strains are elastic.

The above parameters were compared to the mean stress data on axially loaded unnotched specimens in Refs *12* and *27–34*. Parameters *b* and *c* gave fair agreement with the data in most cases, but *a* was often excessively conservative for ductile metals.

Mean Stress and Cycle Counting

To predict the fatigue life for complicated stress-strain histories, it is necessary to use some method of accounting for mean stress in combination with a cycle counting method. An average mean stress is sometimes defined for the entire history [*35*]. If the average mean stress were the significant variable, the stress sequences of Fig. 7*a* and 7*b* would be equally damaging, but this is not likely because *a* has more cycles at a high tensile mean stress. The use of the average mean stress necessitates the assumption that equal numbers of cycles an equal amount above and below the average mean have a cancelling effect. It will be shown experimentally that this is not so.

It has been suggested [*20*, *36*] that the average mean stress be defined for sections of the stress-strain history. Such a procedure could be applied to the sequences of Fig. 7, but for more irregular histories arbitrary divisions of the history into sections would have to be made. The life predictions could vary considerably depending on how the history is divided into sections and also on how the mean stress within each section is defined.

None of these difficulties are encountered if the mean stress of each cycle is determined. This is conveniently done when cycles are defined according to the rain flow counting method, the mean stress of each cycle being simply the average of the most positive and most negative stress peaks occurring during that cycle.

Predicting Cyclic Stress-Strain Response

If the strain history at the location critical for fatigue failure is known, the stress history can be estimated. If the rain flow cycle counting method is applied to the strain history, the strain ranges which form closed stress-strain hysteresis loops, and those few strain ranges which do not, are identified. Stable stress-strain hysteresis loops from low cycle fatigue tests or the results of an incremental step test [*37*] can then be used to estimate the stress history. A computer simulation of the response of the material during cyclic loading could also be used to estimate the stress history. Martin et al [*38*] have successfully employed such a computer program for 2024-T4 aluminum, and their general approach is applicable to other metals.

In situations where a known load or nominal strain history causes plastic straining at a stress concentration, the fatigue life can be predicted if the local stresses and strains at the stress concentration can be estimated [*1*, *38–43*]. Tucker [*44*] has developed a procedure for predicting the fatigue failure of notched parts subject to service loadings by using the simulated cyclic response of the material and Neuber's rule to estimate the local stresses and strains at the notch.

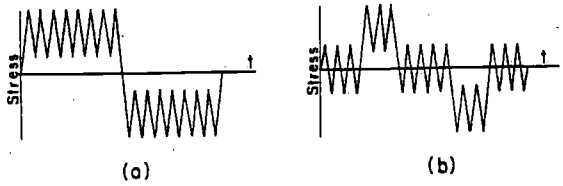

FIG. 7—*Two sequences which have the same average mean stress.*

Proposed Cumulative Damage Procedure

If both the strain history and the stress history at the location critical for fatigue failure are known or can be estimated, and if axial strain versus cycles to failure data for prestrained and nonprestrained specimens are available, the following cumulative damage procedure is recommended:

1. Apply the rain flow counting method to the strain history.
2. Use the stress history to determine the mean stress for each cycle defined by the rain flow counting method. Convert each cycle that has a significant mean stress to an equivalent completely reversed cycle by means of a mean stress parameter. If mean stress data are available for the material being used, these data may be used instead of a mean stress parameter.
3. Sum cycle ratios separately over the initiation and propagation periods based on the assumption that a few cycles of plastic prestraining cause crack initiation. Specifically, assume that the initiation period ends when $\sum(n/N_o) = 1$, the N_o value for a given strain range being equal to $N_f - N_p$. Next sum damage using the strain-life curve for prestrained specimens. Failure is predicted when $\sum(n/N_p) = 1$. For strain ranges too large for there to be a significant effect of prestrain, use $N_p = N_f$. Note that if significant plastic straining occurs near the beginning of the test, the initiation period is short and can be ignored.

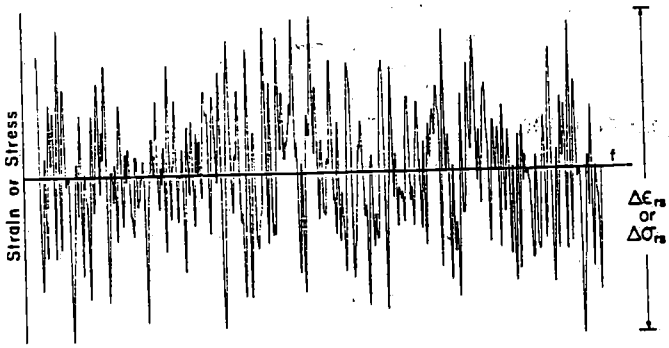

FIG. 8—*The random sequence.*

General Description of Tests

Axially loaded unnotched specimens of 2024-T4 aluminum with cylindrical test sections having nominal diameters of 0.25 in. and lengths of 0.65 in. were tested. The specimens were machined from ¾-in. rods of 2024-T4 which were purchased at the same time as those used in Refs *12*, *13*, *38*, and *45*. The tensile properties, cyclic properties, composition, and source of this metal are given in Ref *45*.

All tests were conducted on an MTS closed loop axial hydraulic materials testing system. Strains were measured over a gage length of 0.55 in. using an Instron clip gage. The tests were conducted in either strain control or stress control, and both the stresses and the strains were recorded for the duration of all tests.

In addition to the function generator that normally controls the testing system, a second function generator was employed so that two superimposed signals of different frequencies could be used as the control signal. A Hewlett-Packard Model 3722A noise generator at a setting of $n = 11$ was used to control some of the tests. This output, which consists of a sequence of approximately 200 peaks that is repeated continuously, is shown in Fig. 8 and will be referred to as the random sequence. An electronic switching and delay circuit was used so that the static stress level could be changed at intervals of one or more repetitions of the random sequence.

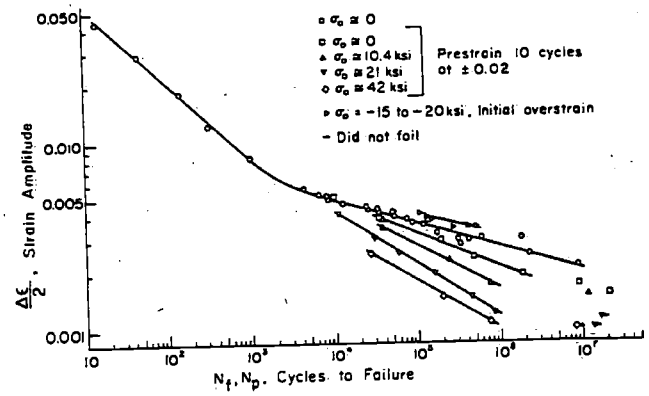

FIG. 9—*Fatigue data from Refs* 12 *and* 45 *for 2024-T4 aluminum.*

Ninety-eight specimens were tested to failure using a variety of strain or stress control conditions. These tests were conducted in twelve groups. In each group one or two test parameters were varied while the others were held constant. Within each group the tests were conducted in arbitrary order to avoid the possibility of systematic errors appearing as trends in the data.

In all but the first group, the test results are compared to the fatigue lives predicted[2] using the proposed cumulative damage procedure. The predictions were based on the data from Refs *12* and *45*, which are shown in Fig. 9. To predict the fatigue lives for some of the strain control tests, it was necessary to estimate the stable mean stresses. This was done using the rain flow counting method and the cyclically stabilized incremental step test result shown in Fig. 10.

Test Results and Discussion

Under this heading each group of tests is described and the results are presented and discussed. The effect of prestrain is investigated and the possible causes of this effect are explored. Next, two groups of tests relating to the cause of the mean stress

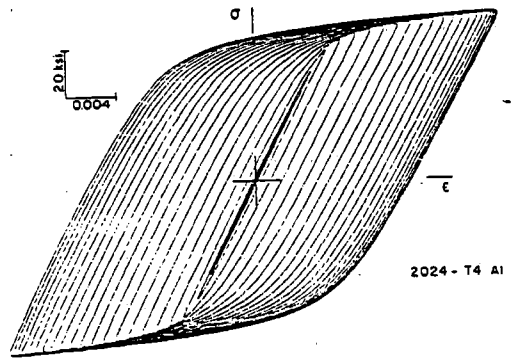

FIG. 10—*Stress-strain record for incremental step test.*

[2] For each group of tests, the predictions were made before any tests in that group were conducted. Note that this is contrary to common practice in cumulative damage studies, which is to conduct the tests and then make fatigue life calculations, adjusting parameters until there is agreement with the actual fatigue lives.

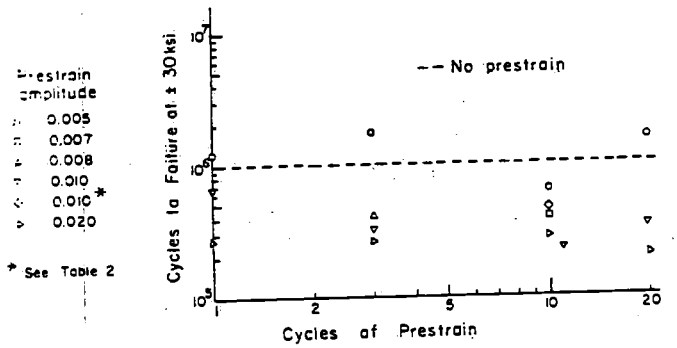

FIG. 11—*Effect of number of cycles and amplitude of prestrain.*

effect are discussed. Block size effects are shown to exist for histories with significant plastic strains and for histories with predominantly elastic strains. The next subheading is concerned with complicated histories in strain control during which large plastic strains occur. Finally, four groups of stress control tests which have programmed variations of the static stress are discussed.

Effect of Prestrain

A number of specimens were prestrained 1, 3, 10, or 20 cycles at various amplitudes of prestrain and were then cycled to failure under stress control at ±30 ksi. These data are shown in Fig. 11 and Table 2, and some examples of the stress-strain response during prestraining are shown in Figs. 12*a* and 12*b*. The specimens prestrained at ±0.005 generally required a greater number of cycles for failure than did those prestrained at larger amplitudes. Other than this, there are no significant trends with either number of cycles or amplitude of prestrain, the bulk of the data lying in a scatterband roughly symmetrical about 3.5×10^5 cycles.

The effect of prestrain could be due to causes other than crack initiation. Slight buckling of the specimen during the compressive portion of the prestrain cycles could reduce the subsequent fatigue life due to superimposed bending stresses. The fatigue life would be expected to be shorter both for greater prestrain amplitude and number of cycles, but the data do not show this. Cyclic hardening during prestraining could reduce the amount

TABLE 2—*Effect of number of cycles and amplitude of prestrain.*

Prestrain Amplitude	Cycles of Prestrain	Cycles to Failure at ±30 ksi
0.0050	1	1 224 500
0.0050	3	1 722 700
0.0050	10	629 900
0.0050	20	1 516 700
0.0070	10	390 400
0.0080	3	409 800
0.0100	1	668 900
0.0100	10[a]	462 900
0.0100	11	230 100
0.0100	20	340 200
0.0103	3	328 800
0.0200	1	274 200
0.0200	3	267 700
0.0200	10	281 300
0.0200	20	207 500

[a] Strain amplitude linearly decreased to zero during cycles 10 to 20.

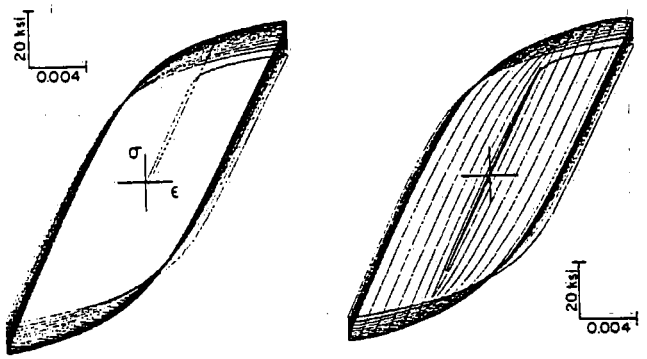

(a) Twenty cycles at ±0.01

(b) Ten cycles at ±0.01, then linearly decrease Δε to zero

FIG. 12—*Examples of stress-strain response during prestraining.*

of plastic strain that occurs during the subsequent cycling, but this should cause prestraining to have a beneficial effect rather than the observed detrimental effect.

If the effect of prestrain were due to the removal of compressive surface residual stresses induced during fabrication [*12*], the specimens prestrained at ±0.005 should have had fatigue lives similar to the others. That an amplitude of ±0.005 is sufficient to remove residual stresses was verified by preloading a specimen to a compressive stress of 35 ksi (see Fig. 13) to simulate a residual stress of that value. The specimen was then cycled under strain control for 10 cycles at ±0.0048 about the new strain zero and the resulting mean stress was observed to be 3.6 ksi in compression, which is insignificant compared with the original value.

Unloading from near the tip of a hysteresis loop after cycling at a large strain amplitude can cause a surface residual stress [*46*] which is compressive for unloading from tension. On one of the specimens the strain amplitude was gradually reduced to zero after prestraining (see Fig. 12*b*) to avoid any compressive residual stress. The subsequent fatigue life was not less than for the other prestrained specimens, as would be expected if residual stresses induced by unloading after prestraining were significantly affecting the fatigue lives.

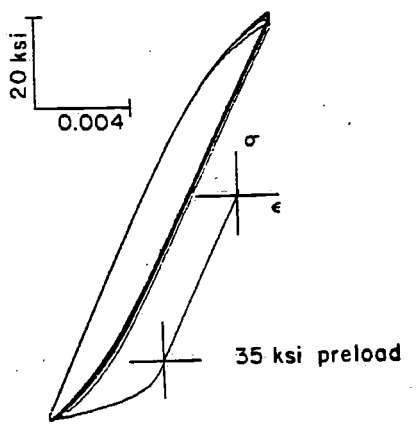

FIG. 13—*Simulated removal of residual stress by prestraining 10 cycles at ±0.0048.*

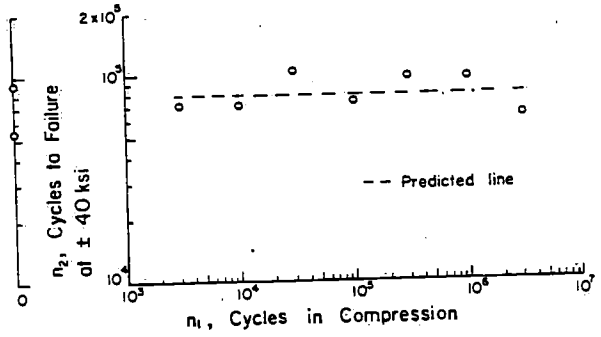

FIG. 14—*Fatigue lives at ±40 ksi after cycling in compression 0 to −50 ksi.*

The test data are consistent with the assumption that prestraining causes damage to the material that could be attributed to the initiation of a crack. There was no evidence that buckling, cyclic hardening, or residual stresses cause the prestrain effect for 2024-T4 aluminum.

Cause of Mean Stress Effect

It was proposed by Takao and Endo [47] that crack initiation depends only on the amplitude of shear stress, mean stress having no effect. Since a tensile stress is thought to be necessary for crack propagation, compressive cycling should initiate a crack without causing any additional damage. Specimens that had been cycled in compression a sufficient number of cycles could then be tested to failure at different mean stresses. The results could be used to determine the effect of mean stress on the lengths of the initiation and propagation periods.

Seven specimens of 2024-T4 were cycled from zero to 50 ksi in compression for various numbers of cycles and were then cycled to failure at ±40 ksi. These data are shown in Fig. 14 and Table 3. Note that the numbers of cycles to failure at ±40 ksi are in close agreement with the lives of two specimens which had no compressive cycles applied and also with the fatigue life from Fig. 9 for nonprestrained specimens, 8.0×10^4 cycles. There was no tendency for the fatigue lives to be reduced to that for prestrained specimens, 3.5×10^4 cycles, even though as many as 3×10^6 compressive cycles were applied.

The compressive cycles, therefore, caused no significant fatigue damage. A greater number of compressive cycles or a larger compressive stress might have caused significant damage. Greater numbers of compressive cycles were not applied because of the excessive testing time necessary. A larger compressive

TABLE 3—*Fatigue lives at ±40 ksi after cycling in compression.*[a]

Cycles in Compression, n_1	Cycles to Failure at ±40 ksi, n_2	Summation of Cycle Ratios, $\Delta(n/N_f)$
0	54 000	0.68
0	90 900	1.14
3 000	71 300	0.89
10 000	70 900	0.88
30 000	105 300	1.32
100 000	74 200	0.93
300 000	98 000	1.23
1 000 000	96 400	1.20
3 000 000	63 200	0.79

[a] During the first 100 to 200 compressive cycles, the minimum stress was gradually decreased to −50 ksi as the specimen hardened. By this procedure the accumulated plastic strain during the compressive cycling was limited, the measured values all being between 0.0055 and 0.0075.

TABLE 4—*Effect of overload cycles on the fatigue lives at different mean stresses.*[a]

Mean Stress, σ_0, ksi	Cycles between Overloads	Type Overload, ksi	Cycles at $\Delta\sigma$ = 50 ksi to Failure	Summation of Cycle Ratios, $\Delta(n/N_p)$
−10	200 000	±60	>10 000 000	...
0	30 000	±60	630 000	1.05
10	10 000	±60	131 600	0.66
20	4 000	±60	69 600	0.87
35	2 000	±60	34 000	0.85
0	30 000	−60	900 000	1.50
10	10 000	−60	133 000	0.67
20	4 000	−60	65 900	0.82

[a] All specimens were prestrained 10 cycles at ±0.012 similar to Fig. 12b then tested in stress control at $\Delta\sigma$ = 50 ksi.

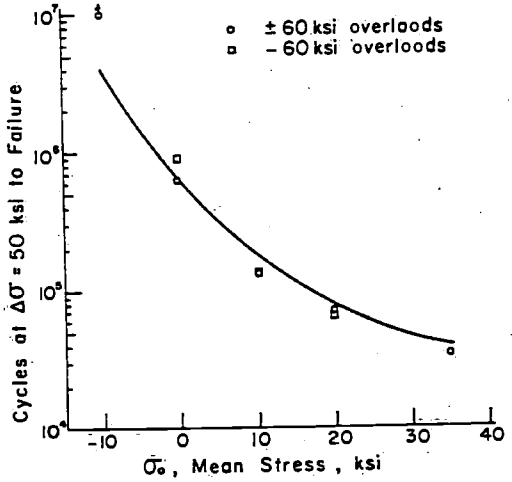

(a) Test data and predicted line

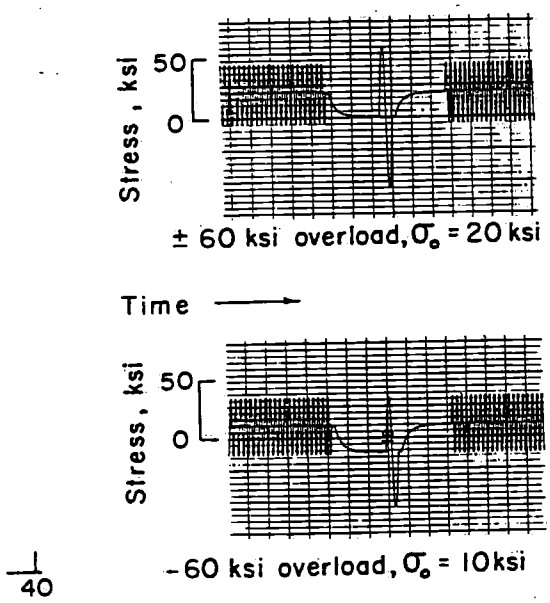

(b) Typical overload cycles

FIG. 15—*Effect of overload cycles on the fatigue lives at different mean stresses.*

stress would have resulted in large plastic strains at the beginning of the compressive cycling. With the method proposed in Ref 47, it is neither practical nor possible to determine whether or not mean stress has an effect during crack initiation for 2024-T4 aluminum.

The variations in plastic strain range during the cycling at ±40 ksi were measured for all of the specimens, including the two which received no compressive cycles. The hardening behavior was not significantly affected by the compressive cycling.

Fracture mechanics studies [48] indicate that the size of fatigue crack necessary to cause final failure of a specimen should be smaller for tests in which higher maximum stresses frequently occur. One possible cause of the effect of mean stress is that, for a given constant amplitude, fewer cycles at a tensile mean stress are necessary to cause a crack of critical size than for zero or compressive mean stress simply because the critical crack size is smaller if the maximum stress is more tensile.

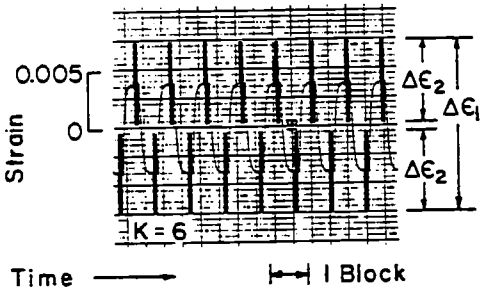

(a) Typical strain–time recordings

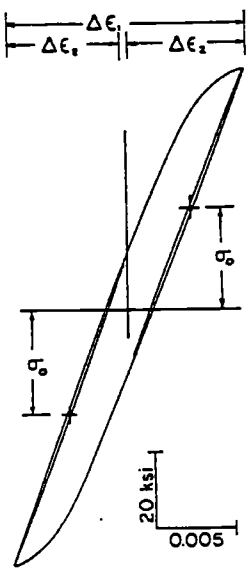

(b) Typical stress–strain response

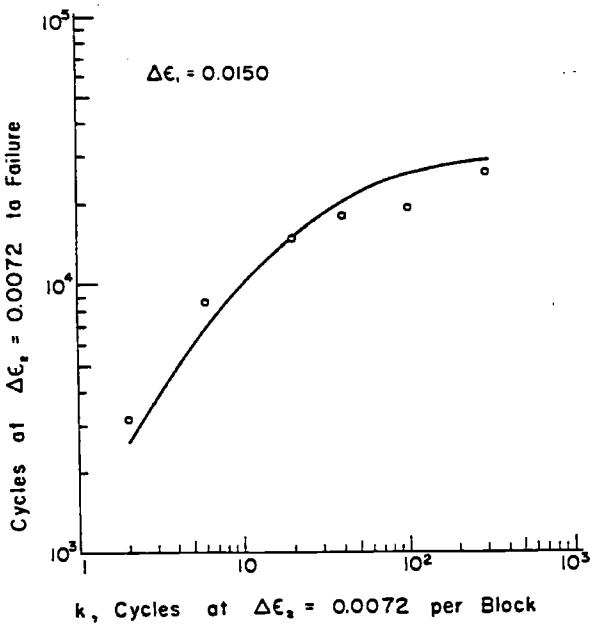

(c) Test data and predicted line

FIG. 16—*Strain control block size effect tests.*

A number of prestrained specimens were tested at the same stress amplitude but at different mean stresses. At intervals of 5 percent of the predicted lives, one cycle at ±60 ksi was applied to exclude any effect of critical crack size. The results of these tests are given in Fig. 15 and Table 4. All of the specimens overloaded at ±60 ksi would have had similar fatigue lives if the effect of mean stress is due solely to the critical crack size. But the overload cycles, and therefore the critical crack size, had no significant effect on the fatigue lives.

Tensile overload cycles could increase the fatigue life by causing crack blunting [49] or local compressive residual stresses [50], and compressive overloads could have the opposite effect. Tensile overloads alone could therefore obscure the effect of critical crack size. It was for this reason that the tensile overloads were followed by compressive overloads. For comparison, three specimens were tested with overloads of −60 ksi (see Table 4 and Fig. 15). As neither the overloads at ±60 ksi nor

TABLE 5—*Strain control block size effect tests.*[a]

Cycles at $\Delta\epsilon_1 = 0.0072$ per Block, k	Cycles at $\Delta\epsilon_1 = 0.0072$ to Failure	Summation of Cycle Ratios, $\Sigma(n/N_p)$
2	3 160	1.21
6	8 580	1.29
20	14 750	1.00
40	17 800	0.89
100	19 200	0.75
300	25 800	0.89

[a] The mean strain was alternated from +0.0039 to −0.0039 at intervals of $k/2$ cycles at $\Delta\epsilon_1$, giving a total strain range of $\Delta\epsilon_1 = 0.0150$.

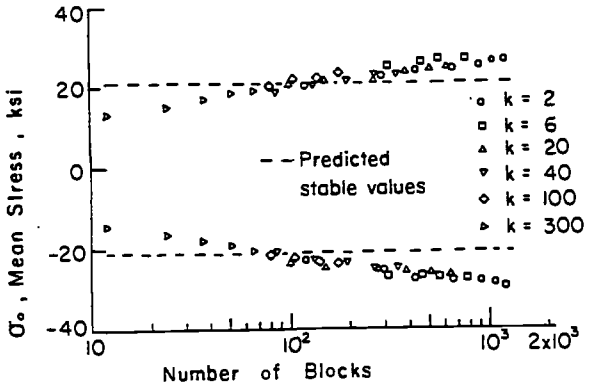

FIG. 17—*Variations in mean stress of cycles at $\Delta\epsilon_2 = 0.0072$ during strain control block size effect tests.*

those at −60 ksi had a significant effect on the fatigue lives, no evidence was found that either crack sharpening/blunting or local residual stresses are important for the specimens used here.

Mean stress could affect the fatigue life by changing the stable stress-strain hysteresis behavior. For hysteresis loops with a given strain range, no dependence of the stress or plastic strain ranges on mean stress was observed in preliminary tests. Similar observations will be made for some of the complicated history tests to be described.

Block Size Effect

One group of tests was conducted in strain control with the mean strain changed alternately between equal positive and

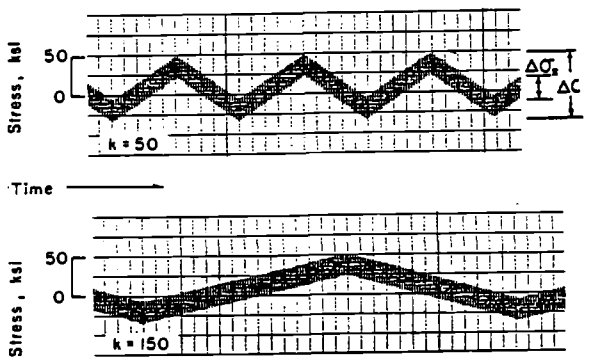

(a) Typical stress – time recordings

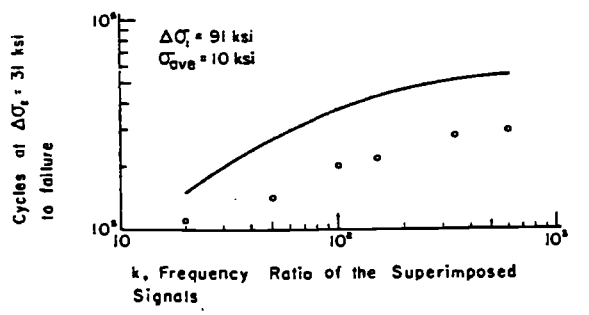

(b) Test data and predicted line

FIG. 18—*Stress control block size effect tests.*

TABLE 6—*Stress control block size effect tests.*[a]

Cycles at $\Delta\sigma_2$ = 31 ksi per Block, k	Cycles at $\Delta\sigma_2$ = 31 ksi to Failure	Summation of Cycle Ratios, $\Sigma(n/N_p)$
20	110 000	0.73
50	141 000	0.52
100[b]	201 000	0.54
150	213 000	0.50
340[b]	278 000	0.55
600	293 000	0.54

[a] The mean stress was varied in a triangular wave about +10 ksi at an amplitude of 30 ksi, giving a total stress range of $\Delta\sigma_1$ = 91 ksi.

[b] The specimens for which k = 100 and 340 were prestrained 10 cycles at ±0.012 similar to Fig. 12b. For all of the others, $\Delta\sigma_2$ was gradually increased to the test value as the specimen hardened during the first few blocks. This resulted in a mean strain of approximately 0.02 that did not increase measurably until the last 5 percent of the fatigue life.

negative values. Between each change of the mean strain a number of cycles was applied, this number being varied for different specimens. Typical strain-time recordings, typical stress-strain behavior, and plotted test results are given in Fig. 16. The tabular results are given in Table 5. The test results are seen to be in excellent agreement with the curve predicted by the proposed cumulative damage procedure. When k, the number of cycles per block at $\Delta\epsilon_2 = 0.0072$, was large, the cycles

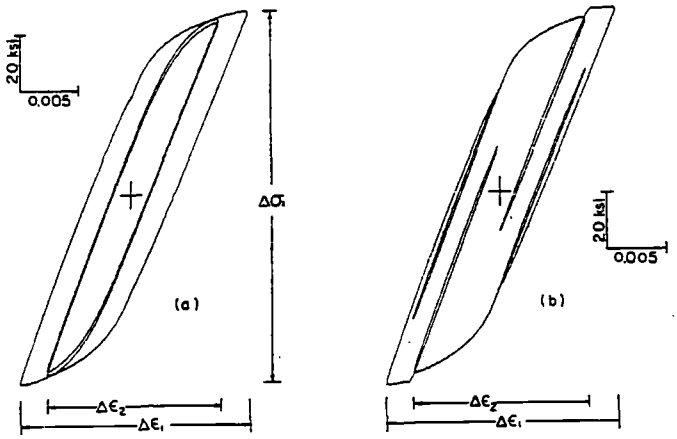

(a) and (b) Stress-stroin response for sequences shown in Fig. 6 (a) and (b)

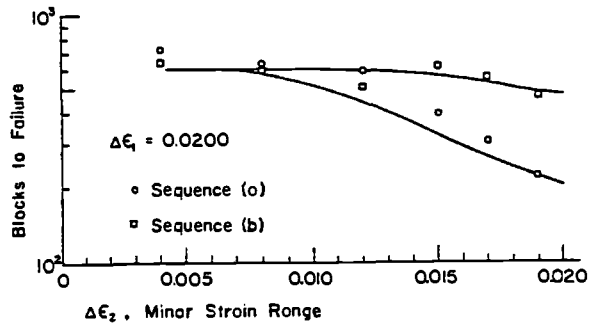

(c) Test data and predicted lines

FIG. 19—*Strain control memory effect tests.*

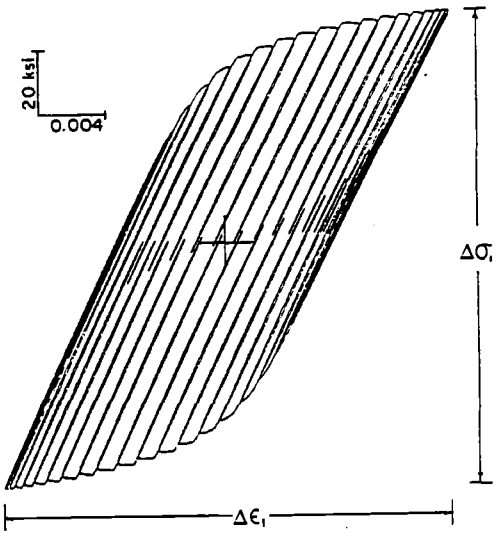

(a) Stable stress-strain response for $\Delta\epsilon_1 = 0.0270$

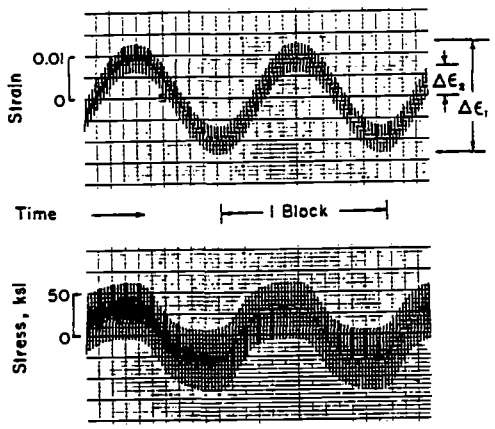

(b) Strain – time and stress – time recordings for $\Delta\epsilon_1 = 0.027$

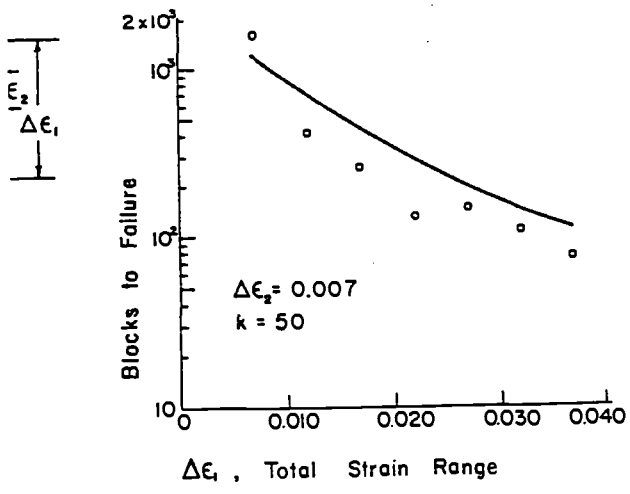

(c) Test data and predicted line

FIG. 20—*Tests with sinusoidal variation of the mean strain.*

TABLE 7—*Strain control memory effect tests.*

Minor Strain Range, $\Delta\epsilon_2$	Sequence[a]	Blocks to Failure	Summation of Cycle Ratios, $\Sigma(n/N_p)$
0.0040	(a)	721	1.20
0.0080	(a)	632	1.10
0.0120	(a)	590	1.34
0.0150	(a)	395	1.22
0.0170	(a)	304	1.15
0.0190	(a)	220	1.00
0.0040	(b)	639	1.06
0.0080	(b)	591	0.99
0.0120	(b)	507	0.86
0.0150	(b)	612	1.08
0.0170	(b)	553	1.04
0.0190	(b)	467	0.97

[a] Sequences (a) and (b) refer to Figs. 6*a* and 6*b*, respectively.

at $\Delta\epsilon_1 = 0.0150$ that occurred one per block were too infrequent to have a significant effect. At small values of k the number of cycles to failure at $\Delta\epsilon_2 = 0.0072$ was reduced because the cycles at $\Delta\epsilon_1 = 0.0150$ contributed a major portion of the damage. The block size in a two-level test can thus affect the fatigue life.

The variations in mean stress during the cycles at $\Delta\epsilon_2 = 0.0072$ are plotted in Fig. 17. Life predictions were made using the estimated stable value of the mean stress shown in Fig. 17. This value is a few ksi smaller than the measured value for most of the tests because slightly more cyclic hardening occurred than was predicted using Fig. 10. After cyclic stabilization in all tests, the mean stress relaxed about 1 ksi following each change of the mean strain.

A similar block size effect can also occur where the strains are essentially elastic, as is illustrated by the next group of tests. Stress control with an input signal consisting of a sine wave superimposed on a triangular wave of lower frequency was employed. Typical stress-time recordings are shown in Fig. 18*a*, and the results of these tests are given Fig. 18*b* and Table 6. The data show a trend similar to the predicted line, but there was a tendency for failures to occur at about half the predicted lives.

Low Cycle Fatigue with Complicated Strain Histories

Three groups of strain control tests were conducted in which strain ranges on the order of 0.02 or 0.03 were imposed. The

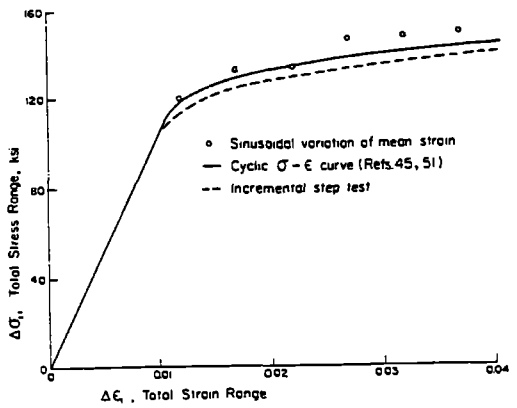

FIG. 21—*Total strain range versus total stress range after cyclic stabilization for sinusoidal variation of the mean strain.*

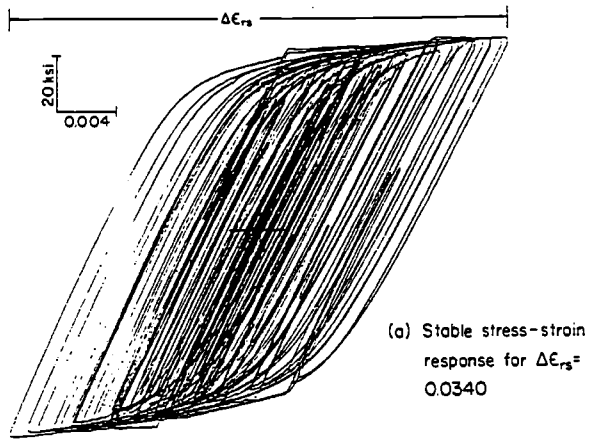

(a) Stable stress-strain response for $\Delta\epsilon_{rs}$ = 0.0340

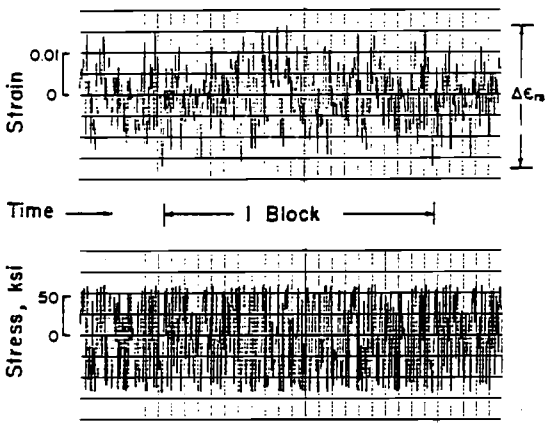

(b) Strain – time and stress – time recordings for $\Delta\epsilon_{rs}$ = 0.0340

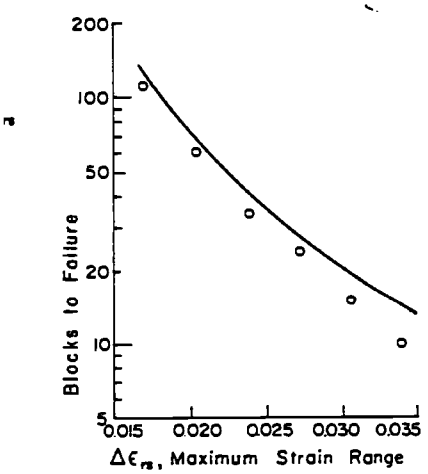

(c) Test data and predicted line

FIG. 22—*Strain control random sequence tests.*

first of these is illustrated in Figs. 6 and 19*a* and 19*b*. By changing the sequence of the strain peaks, the stress-strain behavior was altered. Note that more plastic straining occurs for *a* than for *b*. This difference is caused by the fact that the metal behaves differently depending on the sign of the previous large strain peak that is, there is a memory effect.

TABLE 8—*Tests with sinusoidal variation of the mean strain.*[a]

Total Strain Range, $\Delta\epsilon_1$	Blocks to Failure	Summation of Cycle Ratios, $\Sigma(n/N_p)$
0.0070	1 582	1.32
0.0120	414	0.56
0.0170	265	0.62
0.0220	131	0.46
0.0270	149	0.73
0.0320	109	0.73
0.0370	74	0.67

[a] For all tests $\Delta\epsilon_2 = 0.0070$ and $k = 50$.

Tests were conducted using different values of $\Delta\epsilon_2$ (defined in Fig. 6) while $\Delta\epsilon_1$ was kept constant at 0.020. The results are given in Fig. 19*c* and Table 7. There was a significant difference in the fatigue lives for the two different sequences of straining, and the agreement of the data points with the predicted lines is reasonable. In each of the memory effect tests small closed hysteresis loops were present that had equal strain ranges but different mean stresses. There was never any measureable dependence of the shape of these loops on the mean stress.

Typical stress-strain, strain-time, and stress-time recordings for the second group of low cycle tests are shown in Figs. 20*a* and 20*b*. Two sine waves having frequencies with a ratio of 50 were superimposed to obtain the control signal. The amplitude of the lower frequency wave was varied while that of the higher frequency wave was kept constant. Results for this group of tests are given in Fig. 20*c* and Table 8. The data show the same trend as the predicted line, but the failures usually occurred at 60 or 70 percent of the predicted lives. According to the proposed damage procedure, most of the damage was done by the minor cycles for the smaller values of $\Delta\epsilon_1$ but at the larger values of $\Delta\epsilon_1$ the minor cycles were less important.

In Fig. 21 the stable (half life) values of $\Delta\sigma_1$ are plotted against $\Delta\epsilon_1$. Most of the points lie above the cyclic stress-strain curve, indicating that more cyclic hardening occurred than for simple constant amplitude tests. To predict the fatigue lives for these tests, it was necessary to estimate the mean stress of each small cycle in one block of straining after cyclic stabilization. This was done using the incremental step test of Fig. 10. Stress range versus strain range for this incremental step test is also shown in Fig. 21. The largest mean stresses for each test were underestimated by half the distance between the plotted points and this curve. The line in Fig. 21 for the incremental step test lies slightly below the cyclic stress-strain curve. It is likely that the

TABLE 9—*Strain control random sequence tests.*

Maximum Strain Range, $\Delta\epsilon_{rs}$	Blocks to Failure	Summation of Cycle Ratios, $\Sigma(n/N_p)$
0.0170	111	0.88
0.0204	60	0.90
0.0238	34	0.83
0.0272	24	0.89
0.0306	15	0.78
0.0340	10	0.69

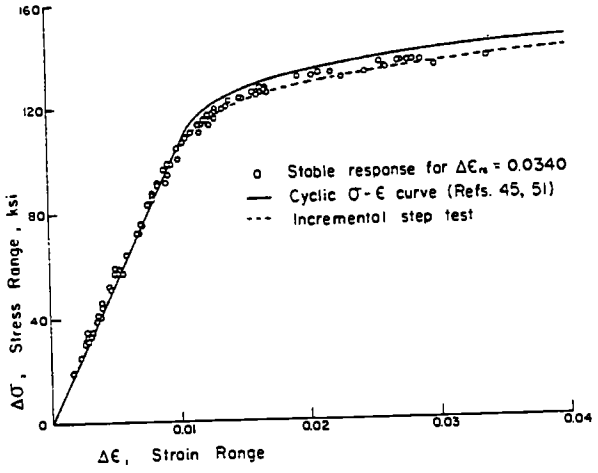

FIG. 23—*Stress range versus strain range for closed hysteresis loops during strain control random sequence tests.*

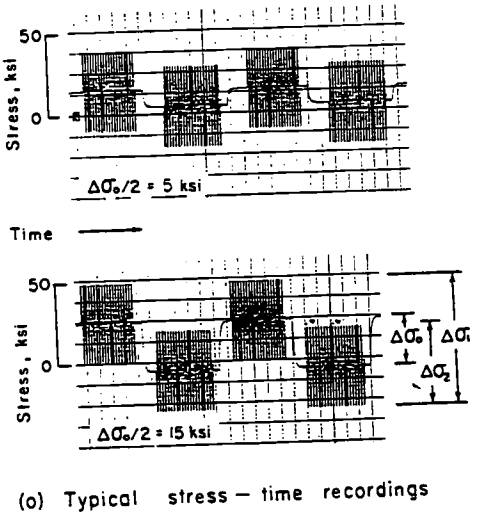

(a) Typical stress — time recordings

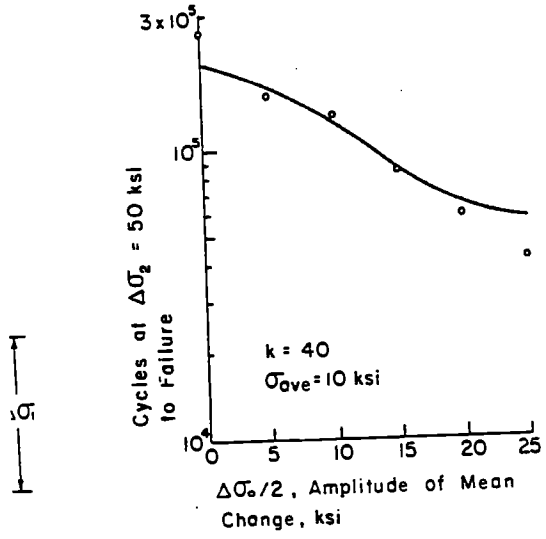

(b) Test data and predicted line

FIG. 24—*Constant average mean stress tests.*

TABLE 10—*Constant average mean stress tests.*[a]

Amplitude of Mean Change about +10 ksi, $\Delta\sigma_0/2$, ksi	Total Stress Range, $\Delta\sigma_1$, ksi	Cycles at $\Delta\sigma_2$ = 50 ksi to Failure	Summation of Cycle Ratios, $\Sigma(n/N_p)$
0	50	259 900	1.30
5	60	155 800	0.93
10	70	132 300	1.06
15	80	84 600	0.99
20	90	59 600	0.91
25	100	41 400	0.73

[a] All specimens were prestrained 10 cycles at ±0.012 similar to Fig. 12*b*. The mean stress was alternated from 10 + $\Delta\sigma_0/2$ to 10 − $\Delta\sigma_0/2$ at intervals of 20 cycles at $\Delta\sigma_2$ = 50 ksi.

specimen used for this test was of slightly less than average hardness, because other incremental step test results for 2024-T4 aluminum [*37*, *51*] are in closer agreement with the cyclic stress-strain curve.

Note in Fig. 20*a* that the plastic strain range during minor

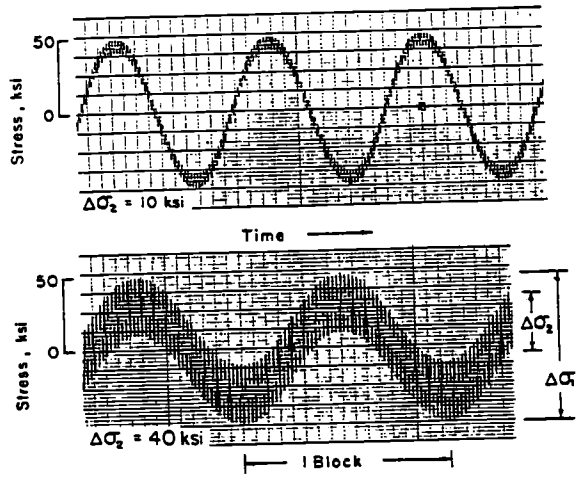

(a) Typical stress — time recordings

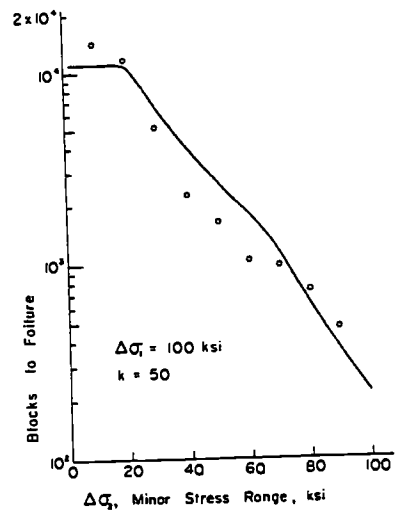

(b) Test data and predicted line

FIG. 25—*Tests with sinusoidal variation of the mean stress.*

cycles is not dependent on the mean stress. Similar observations were made for the other tests in this group.

The third group of low cycle tests employed the random sequence (Fig. 8) as the strain control signal. The random sequence was repeatedly applied and was attenuated, but not distorted, by various amounts to give different values of $\Delta\epsilon_{rs}$.

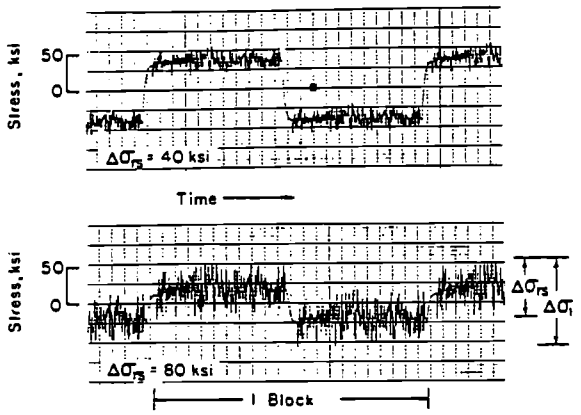

(a) Typical stress-time recordings

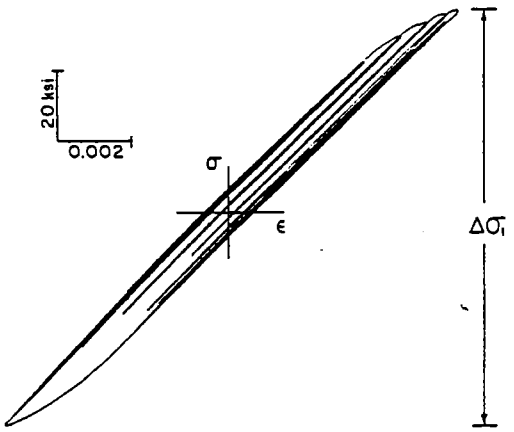

(b) Stable stress-strain response for $\Delta\sigma_{rs}$ = 100ksi

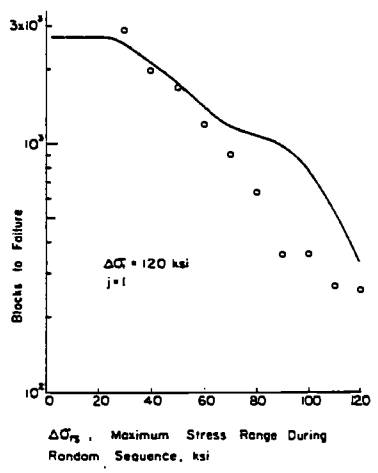

(c) Test data and predicted line

FIG. 26—*Stress control random sequences at two static levels.*

TABLE 11—*Tests with sinusoidal variation of the mean stress.*[a]

Minor Stress Range, $\Delta\sigma_2$, ksi	Blocks to Failure	Summation of Cycle Ratios, $\Sigma(n/N_p)$
10	14 200	1.29
20	11 750	1.07
30	5 160	0.78
40	2 280	0.56
50	1 660	0.63
60	1 050	0.54
70	977	0.84
80	738	1.18
90	468	1.30

[a] All specimens were prestrained 10 cycles at ±0.012 similar to Fig. 12*b*. For all tests $\Delta\sigma_1$ = 100 ksi and k = 50.

Typical stress-strain, strain-time, and stress-time recordings are shown in Figs. 22*a* and 22*b* and the test results in Fig. 22*c* and Table 9. The test results are in excellent agreement with the predicted line.

For one of the strain control random tests, the strain ranges counted as cycles by the rain flow counting method, which are the strain ranges for all closed hysteresis loops, are plotted against the corresponding stable stress ranges in Fig. 23. The plotted points lie slightly but not significantly below the cyclic stress-strain curve. Similar plots for several of the other strain control random block tests showed similar or better agreement with the cyclic stress-strain curve.

Complicated Histories with Periodic Variation of the Mean Stress

Four groups of tests were conducted in stress control with programmed periodic changes in the static stress level. All specimens were prestrained 10 cycles at ±0.012 similar to Fig. 12*b*. If the specimens had not been intentionally prestrained, large plastic strains would have occurred during cyclic hardening for most of the tests.

In the first group of tests an average mean stress of 10 ksi was used with the mean stress varied in a square wave about 10 ksi, different amplitudes of variation being used for different specimens. Forty cycles at a stress range of 50 ksi were applied during each cycle of the mean stress. Typical stress histories are shown in Fig. 24*a*. The test results are shown in Fig. 24*b* and Table 10. The predicted and actual fatigue lives did not differ by more than 30 percent.

TABLE 12—*Stress control random sequences at two static levels.*[a]

Maximum Stress Range during Random Sequence, $\Delta\sigma_{rs}$, ksi	Blocks to Failure	Summation of Cycle Ratios, $\Sigma(n/N_p)$
30	2 892	1.14
40	1 976	0.93
50	1 688	0.96
60	1 189	0.85
70	898	0.76
80	632	0.59
90	355	0.36
100	358	0.46
110	269	0.50
120	257	0.77

[a] All specimens were prestrained 10 cycles at ±0.012 similar to Fig. 12*b*.

If equal numbers of cycles an equal amount above and below the average mean stress have cancelling effects, the fatigue lives for all of the specimens would have been similar to the fatigue life for the specimen that was tested at a constant mean of 10 ksi. The dominant effect was that the cycles at the high tensile mean stress shortened the fatigue lives. Note that the use of the average mean stress to make the life predictions would have resulted in significant nonconservative errors for any variation of the mean greater than ±5 ksi.

Stress histories for the next group of tests are shown in Fig. 25*a*. Two sine waves having frequencies with a ratio of 50 were superimposed so that the peak tensile and compressive stresses in each block were +50 ksi and −50 ksi, respectively. The results of these tests are given in Fig. 25*b* and Table 11. Where $\Delta\sigma_2$ was small, the minor cycles were predicted to have little effect and the fatigue damage for each block was calculated to be the same as for one cycle at ±50 ksi. For $\Delta\sigma_2$ near 100 ksi, the calculated damage per block approaches the value for 50 cycles at ±50 ksi. At small and large values of $\Delta\sigma_2$ the test results and predictions are in excellent agreement, but for intermediate values there was a tendency for the failures to occur at about half of the predicted lives.

In another group of stress control tests the static level was changed between equal tensile and compressive values with one random sequence (see Fig. 8) applied for each change in level. Typical stress-time and stress-strain recordings are shown in Figs. 26*a* and 26*b*, and the test results are given in Fig. 26*c* and Table 12. The quantity $\Delta\sigma_1$ was kept constant at 120 ksi and $\Delta\sigma_{rs}$ was varied over a wide range. Agreement between the actual and predicted fatigue lives is good except for $\Delta\sigma_{rs}$ between 80 and 110 ksi, where there was a tendency for failure at summations of cycle ratios around 0.4 or 0.5.

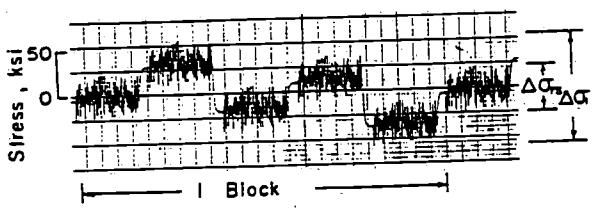

(a) Stress - time record for j=1

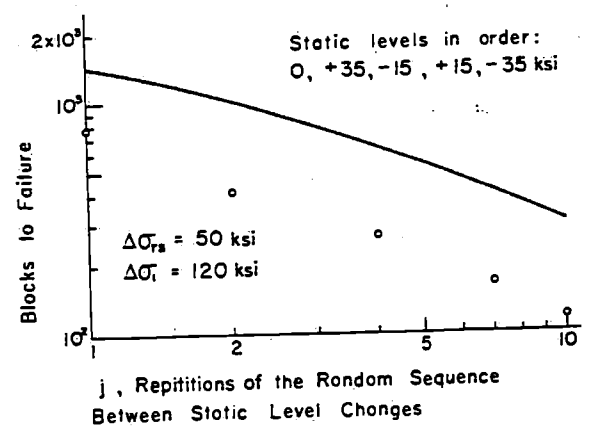

(b) Test data and predicted line

FIG. 27—*Stress control random sequences at five static levels.*

TABLE 13—*Stress control random sequences at five static levels.*[a]

Repetitions of the Random Sequence between Static Level Changes, j	Blocks to Failure	Summation of Cycle Ratios, $\Sigma(n/N_p)$
1	781	0.55
2	405	0.41
4	263	0.42
7	164	0.41
10	117	0.40

[a] All specimens prestrained 10 cycles at ±0.012 similar to Fig. 12*b*. The static stress level was alternated within each block as follows: 0, +35, −15, +15, and −35 ksi.

The final group of tests employed the random sequence at five different static levels as shown in Fig. 27*a*. At each level the random sequence was repeated a number of times. The number of repetitions was the same for all levels of each test but was varied for different tests. Values of $\Delta\sigma_1$ = 120 ksi and $\Delta\sigma_{rs}$ = 50 ksi were used in all of the tests. As it had been noticed from the other test groups that the largest differences between the actual and predicted lives occurred where there were superimposed loadings and predominantly elastic behavior, this group of tests was designed as an extreme case of that situation. The test results in Fig. 27*b* and Table 13 show that the data have a trend similar to the predictions and that summations of cycle ratios near 0.4 were obtained.

Conclusions

The following specific conclusions are supported by the test data on 2024-T4 aluminum:

1. For prestrains larger than ±0.005, the effect on the subsequent fatigue life is not dependent on the number of cycles or amplitude of prestrain. The effect of prestrain is consistent with the assumption that prestraining causes crack initiation. The effect is not caused by cycle-dependent buckling, cyclic hardening, or residual stresses.
2. No significant fatigue damage was caused by as many as 3×10^6 cycles from 0 to −50 ksi, which is approximately the largest compressive stress that can be applied without causing large plastic strains near the beginning of the test.
3. There was no evidence that the effect of mean stress on fatigue life is due to the inverse relationship between critical crack size and maximum tensile stress.
4. Significant block size effects exist and are accounted for if damage is calculated for the major cycle that occurs once per block.
5. In tests with complicated histories that cause large plastic strains, the counting of all closed hysteresis loops as cycles by means of the rain flow counting method allows accurate life predictions.
6. In complicated history tests where there were closed hysteresis loops at different mean stresses, no effect of the mean stress on the stable stress-strain hysteresis behavior was detected.
7. The stable stress-strain relationship for closed hysteresis loops during complicated histories is in general agreement with the cyclic stress-strain curve. The largest deviations occurred for the tests with superimposed sine waves in strain

control, where some of the stress ranges were about 5 percent larger than the values from the cyclic stress-strain curve.

8. The use of the average mean stress is an approximation that should be used with extreme caution. It is valid only if the variations in the mean stress are small.

9. Using the rain flow counting method, the strain-life curve for prestrained specimens, and the mean stress of each cycle gives reasonable predictions for the fatigue lives of prestrained specimens subjected to complicated histories where there is a changing mean stress.

10. The use of any method of cycle counting other than the range pair or rain flow methods can result in inconsistencies and gross differences between predicted and actual fatigue lives.

The proposed cumulative damage procedure gives reasonable predictions of the fatigue failure of 2024-T4 aluminum for a wide variety of complicated stress-strain histories. Tests were conducted to investigate all histories which could be devised to deceive the proposed procedure. For the 83 specimens tested to failure for which failure predictions were made, the summations of cycle ratios were all between 0.36 and 1.50. The values are distributed as shown in Fig. 28. Most of the values below 0.60 occurred in situations where there were large changes in the mean stress with superimposed minor cycles for which the calculated damage was significant. The damages due to large transition cycles and the minor cycles superimposed on them simply do not add linearly. This could be due to the details of crack propagation behavior. Another possibility is that during small predominantly elastic cycles the plastic strains, which were too small to be measured by the techniques employed in this investigation, are larger when the mean stress is changing. In situations where there are significant minor cycles superimposed on large changes in the mean stress, an adjustment of a factor of two in life predictions could be made but a more complicated damage procedure is not justified.

To apply the proposed cumulative damage procedure to a new material, it is necessary to have completely reversed strain-life data for prestrained and nonprestrained specimens. Strain-life data at mean stresses other than zero are desirable but not essential. A set of stable hysteresis loops from the low cycle strain-life tests or the result of an incremental step test is needed. A computer simulation of the stable cyclic response of the material would greatly increase the efficiency of the calculations.

Tests on smooth, axially loaded specimens of other engineering metals are needed to evaluate the proposed cumulative damage procedure. For some metals, history or strain rate dependence of the stable stress-strain behavior, or the lack of a stable stress-strain behavior, might necessitate modifications in the proposed procedure.

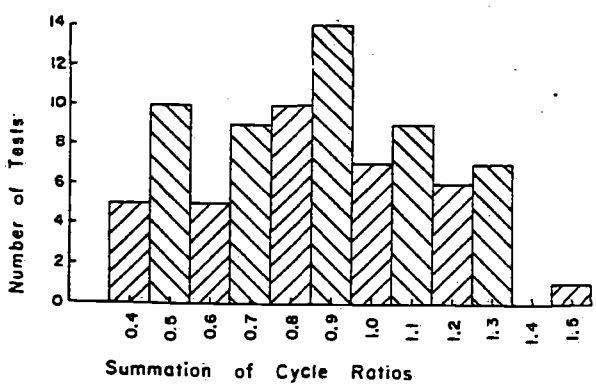

FIG. 28—*Distribution of failure predictions.*

Acknowledgments

This investigation was conducted in the H. F. Moore Fracture Research Laboratory of the Department of Theoretical and Applied Mechanics, University of Illinois, Urbana. Sponsorship was provided by the Naval Air Development Center, Warminster, Pa. F. F. Borriello and R. E. Vining acted as technical liaison for the Navy.

Gratitude is expressed to JoDean Morrow for suggestions, constructive criticisms, and encouragement. The technical aid and advice provided by J. F. Martin is appreciated. The results of this investigation will at a later date become part of a Ph.D. thesis.

APPENDIX

Range Pair and Rain Flow Cycle Counting Methods

The range pair and the rain flow cycle counting methods are described and compared in this Appendix. The apparent complexity of these cycle counting methods disappears after a small amount of practice in applying them. It is suggested that the reader draw some irregular sequences of peaks and apply the range pair and rain flow cycle counting method to them while reading the descriptions below.

Range Pair Counting Method

The range pair counting method counts a strain range as a cycle if it can be paired with a subsequent straining of equal magnitude in the opposite direction. For a complicated history, some of the ranges counted as cycles will be simple ranges during which the strain does not change direction, but others will be interrupted by smaller ranges which will also be counted as cycles. Cycle counting by the range pair method is illustrated in Fig. 29. The counted ranges are marked with solid lines and the paired ranges with dashed lines.

Each peak is taken in order as the initial peak of a range, except that a peak is skipped if the part of the history immediately following it has already been paired with a previously counted range. If the initial peak of a range is a minimum, a cycle is counted between this minimum and the most positive maximum which occurs before the strain becomes more negative than the initial peak of the range. For example, in Fig. 29 a cycle is counted between peak 1 and peak 8, peak 8 being the most positive maximum that occurs before the strain becomes more negative than peak 1. If the initial peak of a range is a maximum, a cycle is counted between this maximum and the most negative minimum which occurs before the strain becomes more positive than the initial peak of the range. For example, in Fig. 29 a cycle is counted between peak 2 and peak 3, peak 3 being the most negative minimum before the strain becomes more positive than peak 2. Each range that is counted is paired with the next straining of equal magnitude in the opposite direction, explaining why complete cycle rather than half cycle counts are made. For example, in Fig. 29 part of the range between peaks 8 and 9 is paired with the range counted between peaks 1 and 8.

Rain Flow Counting Method

The rain flow cycle counting method is illustrated in Fig. 30. The strain-time history is plotted so that the time axis is vertically downward, and the lines connecting the strain peaks are imagined to be a series of pagoda roofs. Several rules are imposed on rain dripping down these roofs so that cycles and half cycles are defined. Rain flow begins successively at the inside of each strain peak. The rain flow initiating at each peak is allowed to drip down and continue except that, if it initiates at a minimum, it must stop when it comes opposite a minimum more negative than the minimum from

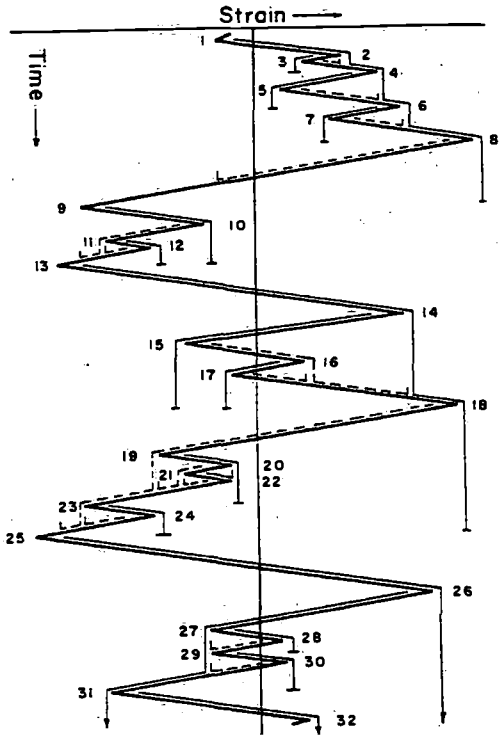

FIG. 29—*Example of range pair cycle counting method.*

which it initiated. For example, in Fig. 30 begin at peak 1 and stop opposite peak 9, peak 9 being more negative than peak 1. A half cycle is thus counted between peaks 1 and 8. Similarly, if the rain flow initiates at a maximum, it must stop when it comes opposite a maximum more positive than the maximum from which it initiated. For example, in Fig. 30 begin at peak 2

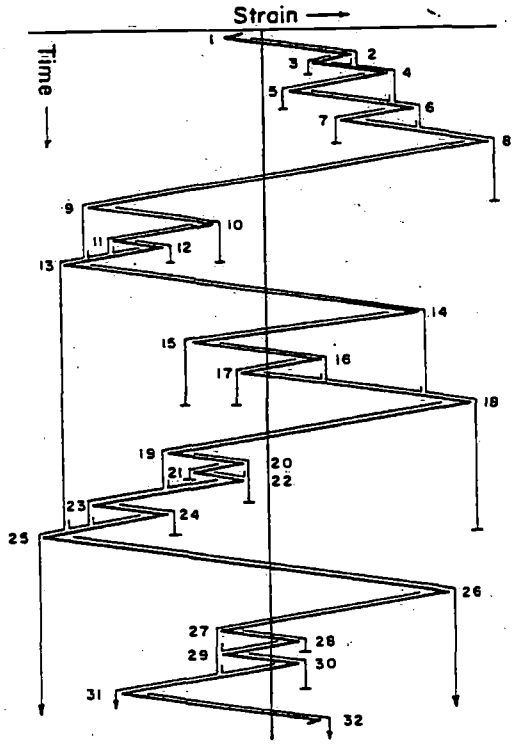

FIG. 30—*Example of rain flow cycle counting method.*

and stop opposite peak 4, thus counting a half cycle between peaks 2 and 3. A rain flow must also stop if it meets the rain from a roof above. For example, in Fig. 30 the half cycle beginning at peak 3 ends beneath peak 2. Note that every part of the strain-time history is counted once and only once.

When this procedure is applied to a strain history, a half cycle is counted between the most positive maximum and the most negative minimum. Assume that of these two the most positive maximum occurs first. Half cycles are also counted between the most positive maximum and the most negative minimum that occurs before it in the history, between this minimum and the most positive maximum occuring previous to it, and so on to the beginning of the history. After the most negative minimum in the history, half cycles are counted which terminate at the most positive maximum occurring subsequently in the history, the most negative minimum occurring after this maximum, and so on to the end of the history. The strain ranges counted as half cycles therefore increase in magnitude to the maximum and then decrease.

All other strainings are counted as interruptions of these half cycles, or as interruptions of the interruptions, etc., and will always occur in pairs of equal magnitude to form full cycles. The rain flow counting method cor-

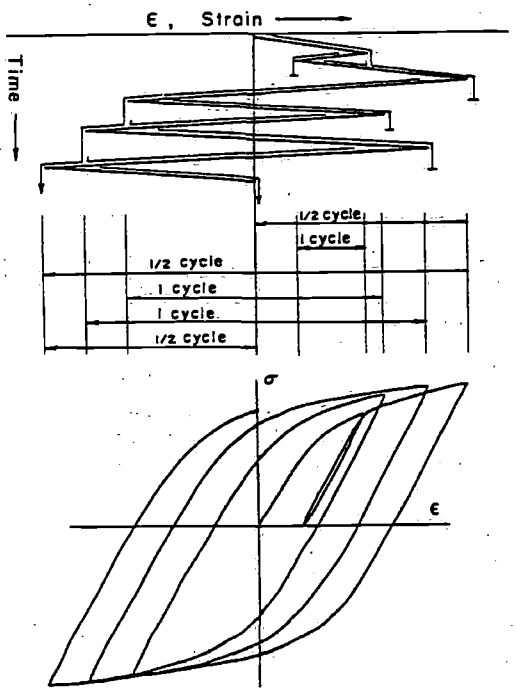

FIG. 31—*Rain flow cycle counting method and stress-strain hysteresis loops.*

responds to the stable cyclic stress-strain behavior of a metal in that all strain ranges counted as cycles will form closed stress-strain hysteresis loops, and those counted as half cycles will not. This is illustrated in Fig. 31.

Comparison of the Range Pair and Rain Flow Cycle Counting Methods

Except when half cycles are being counted, the rain flow counting method reduces to the range pair method. All of the cycles counted by the rain flow method are therefore counted as cycles by the range pair method. But the half cycles counted by the rain flow method are handled differently by the range pair method, resulting in no damage being calculated for some parts of the strain-time history if the range pair method is used. Compare the counting results in Figs. 29 and 30. This difference is significant only in situations where the damage due to individual half cycles is important, namely, where there are only a few reversals to failure or where there are insignificant minor reversals and most of the damage is done by a few major reversals.

If cycles are to be counted for a sequence that is repeated until failure occurs, one complete cycle should be counted between the most positive and most negative peaks in the sequence and other smaller complete cycles

which are interruptions of this largest cycle should also be counted. This will be accomplished by either the rain flow or the range pair cycle counting methods if the cycle counting is started at either the most positive or most negative peak in the sequence. The rain flow method will count no half cycles and will thus give a cycle count identical to that obtained using the range pair method.

The rain flow and range pair cycle counting methods can thus be considered equivalent for most practical situations.

References

[1] Crews, J. H., Jr., and Hardrath, H. F., *Experimental Mechanics*, EXMCA, Vol. 6, No. 6, June 1966, pp. 313–320.

[2] Blatherwick, A. A. and Olson, B. K., *Experimental Mechanics*, EXMCA, Vol. 8, No. 8, Aug. 1968, pp. 356–361.

[3] Hunter, M. S. and Fricke, W. G., Jr., *Proceedings, ASTM*, ASTEA, Vol. 54, 1954, pp. 717–732.

[4] Hunter, M. S. and Fricke, W. G., Jr., *Proceedings, ASTM*, ASTEA, Vol. 56, 1956, pp. 1038–1046.

[5] Hunter, M. S. and Fricke, W. G., Jr., *Proceedings, ASTM*, ASTEA, Vol. 55, 1955, pp. 942–953.

[6] Forsyth, P. J. E. in *Proceedings of the Crack Propagation Symposium*, Vol. I, Cranfield, England, 1961, pp. 76–94.

[7] Hempel, M. in *International Conference on Fatigue on Metals*, IME and ASME, London and New York, 1956, pp. 543–544.

[8] Boettner, R. C., Laird, C., and McEvily, A. J., *Transactions, AIME*, TAIMA, Vol. 233, No. 1, 1965, pp. 379–387.

[9] Hardrath, H. F., "A Review of Cumulative Damage for Fatigue Committee of the Structures and Materials Panel Advisory Group for Aeronautical Research and Development," NASA Langley Research Center, Hampton, Va., June 1965.

[10] Corten, H. T. in *Metals Engineering Design*, ASME Handbook, O. J. Horger, Ed., McGraw-Hill, 1965, pp. 231–241.

[11] Manson, S. S., Freche, J. C., and Ensign, C. R. in *Fatigue Crack Propagation, ASTM STP 415*, American Society for Testing and Materials, 1966, pp. 384–412.

[12] Topper, T. H. and Sandor, B. I. in *Effects of Environment and Complex Load History on Fatigue Life, ASTM STP 462*, American Society for Testing and Materials, 1970, pp. 93–104.

[13] Topper, T. H., Sandor, B. I., and Morrow, J., *Journal of Materials*, JMLSA, Vol. 4, No. 1, March 1969, pp. 189–199.

[14] Ohji, K., Miller, W. R., and Marin, J., *Transactions, ASME*, TASMA, Journal of Basic Engineering, Dec. 1966, pp. 801–810.

[15] D'Amato, R., "A Study of the Strain-Hardening and Cumulative Damage Behavior of 2024-T4 Aluminum Alloy in the Low-Cycle Fatigue Range," WADD TR 60-175, Wright Air Development Center, Ohio, April 1960.

[16] Gucer, D. E., *Transactions Quarterly, ASM*, ASMQA, Vol. 54, No. 2, June 1961, pp. 176–184.

[17] Nakagawa, T. and Nitta, S. in *Proceedings of the Symposium on Fatigue of Metals Under Service Loads*, The Society of Materials Science, Kyoto, Japan, 22 Sept. 1967, pp. 73–83.

[18] Grover, H. J. in *Symposium on Fatigue of Aircraft Structures, ASTM STP 274*, American Society Testing and Materials, 1959, pp. 120–124.

[19] Sinclair, G. M., *Proceedings, ASTM*, ASTEA, Vol. 52, 1952, pp. 743–751.

[20] Jacoby, G. H., "Fatigue Life Estimation Processes Under Conditions of Irregularly Varying Loads," AFML TR 67-215, Air Force Materials Lab., Wright-Patterson AFB, Ohio, Aug. 1967.

[21] Schijve, J. in *Fatigue of Aircraft Structures*, W. Barrios and E. L. Ripley, Eds., Pergamon Press, 1963, pp. 115–148.

[22] Burns, A., "Fatigue Loadings in Flight: Loads in the Tailplane and Fin of a Varsity," Aeronautical Research Council Technical Report C.P. 256, London, 1956.

[23] Matsuishi, M. and Endo, T., "Fatigue of Metals Subjected to Varying Stress," presented at Japan Society of Mechanical Engineers, Fukuoka, Japan, March 1968.

[24] Smith, J. O., "The Effect of Range of Stress on the Fatigue Strength of Metals," Bulletin No. 334, University of Illinois, Engineering Experiment Station, Urbana, Feb. 1942.

[25] Stulen, F. L., "Fatigue Life Data Displayed by a Single Quantity Relating Alternating and Mean Stress," AFML TR 65-121, Air Force Materials Lab., Wright-Patterson AFB, Ohio, July 1965.

[26] Morrow, J., Section 3.2 of *Fatigue Design Handbook*, Society of Automotive Engineers, 1968; Section 3.2 is a summary of a paper presented at a meeting of Division 4 of the SAE Iron and Steel Technical Committee, 4 Nov. 1964.

[27] Smith, K. N., Watson, P., and Topper, T. H., "A Stress-Strain Function for the Fatigue of Metals," Report 21, Solid Mechanics Division, University of Waterloo, Ontario, Canada, Oct. 1969.

[28] Landgraf, R. W., "Effect of Mean Stress on the Fatigue Behavior of a Hard Steel," M.S. thesis, Dept. of Theoretical and Applied Mechanics, University of Illinois, Urbana, 1966; see also T. & A.M. Report 662.

[29] Grover, H. J. et al, "Axial-Load Fatigue Properties of 24S-T and 75S-T Aluminum Alloy as Determined in Several Laboratories," NACA TN 2928, National Advisory Committee for Aeronautics, Washington, D. C., May 1953.

[30] Blatherwick, A. A. and Lazan, B. J., "Fatigue Properties of Extruded Magnesium Alloy ZK 60 Under Various Combinations of Alternating and Mean Axial Stresses," WADC TR 53-181, Wright Air Development Center, Ohio, Aug. 1953.

[31] Lazan, B. J. and Blatherwick, A. A., "Fatigue Properties of Aluminum Alloys at Various Direct Stress Ratios," WADC TR 52-307, Wright Air Development Center, Ohio, 1952.

[32] Howell, F. M. and Miller, J. L., *Proceedings, ASTM*, ASTEA, Vol. 55, 1955, pp. 955–967.

[33] O'Connor, H. C. and Morrison, J. L. M. in *International Conference on Fatigue of Metals*, IME and ASME, London and New York, 1956, pp. 102–109.

[34] Grover, H. J., Bishop, S. M., and Jackson, L. R., "Fatigue Strength of Aircraft Metals: Axial Load Fatigue Tests on Unnotched Sheet Specimens of 24S-T3 and 75S-T6 Aluminum Alloys and of SAE 4130 Steel," NACA TN 2324, National Advisory Committee for Aeronautics, Washington, D.C., March 1951.

[35] Raser, W. H., Jr., in *Metal Fatigue: Theory and Design*, A. F. Madayag, Ed., John Wiley & Sons, 1969, pp. 247–288.

[36] Leve, H. L. in *Metal Fatigue: Theory and Design*, A. F. Madayag, Ed., John Wiley & Sons, 1969, pp. 170–203.

[37] Landgraf, R. W., Morrow, J., and Endo, T., *Journal of Materials* JMLSA, Vol. 4, No. 1, March 1969, pp. 176–188.

[38] Martin, J. F., Topper, T. H., and Sinclair, G. M., *Materials Research and Standards*, MTRSA, Vol. 11, No. 2, Feb. 1971, pp. 23–29.

[39] Manson, S. S. and Hirschberg, M. H. in *Proceedings of the First International Conference on Fracture*, The Japanese Society for Strength and Fracture of Materials, Vol. 1, Sendai, Japan, Sept. 1965, pp. 479–498.

[40] Dolan, T. J. in *Proceedings of the 9th Midwestern Mechanics Conference*, Madison, Wis., Aug. 1965, pp. 3–21.

[41] Wetzel, R. M., *Journal of Materials*, JMLSA, Vol. 3, No. 3, Sept. 1968, pp. 646–657.

[42] Topper, T. H., Wetzel, R. M., and Morrow, J., *Journal of Materials* JMLSA, Vol. 4, No. 1, March 1969, pp. 200–209.

[43] Stadnick, S. J. and Morrow, J., "Techniques for Smooth Specimen Simulation of the Fatigue Behavior of Notched Members," presented at the Mechanical Effects Session of ASTM-NMAB National Symposium on Testing for Prediction of Material Performance in Structures and Components, Anaheim, Calif., 19–24 April 1971.

[44] Tucker, L. E., "A Procedure for Designing Against Fatigue Failure of Notched Parts," M. S. thesis, Dept. of Theoretical and Applied Mechanics, University of Illinois, Urbana, 1970.

[45] Endo, T. and Morrow, J., *Journal of Materials*, JMLSA, Vol. 4, No. 1, March 1969, pp. 159–175.

[46] Taira, S. and Kitagawa, M. in *Symposium on X-Ray Studies of Material Strength*, The Society of Materials Science, Tokyo, Japan, 1966, pp. 84–87.

[47] Takao, K. and Endo, T., "Effect of Mean Stress on the Fatigue Crack Initiation and Propagation of a Carbon Steel," preprint for annual meeting of Japan Society of Mechanical Engineers, No. 203, April 1969, pp. 129–132.

[48] Christensen, R. H. in *Proceedings of the Crack Propagation Symposium*, Vol. II, Cranfield, England, 1961, pp. 326–374.

[49] Rice, J. R. in *Fatigue Crack Propagation, ASTM STP 415*, American Society for Testing and Materials, 1967, pp. 247–309.

[50] Schijve, J. in *Fatigue Crack Propagation, ASTM STP 415*, American Society for Testing and Materials, 1967, pp. 415–457.

[51] Private communication with J. F. Martin concerning the data used in the preparation of Ref *38*, Oct. 1970.